Low Cycle Fatigue Behaviour of Nimonic PE16 Superalloy

M. VALSAN, K. BHANU SANKARA RAO and S. L. MANNAN

Materials Development Laboratory, Indira Gandhi Centre for Atomic Research, Kalpakkam — 603 102, Tamil Nadu, India

ABSTRACT

The influence of microstructure on strain controlled low cycle fatigue behaviour of the Nimonic PE16 superalloy has been studied at a constant strain rate of 3×10^{-3} s^{-1} at 923K in three following microstructural states: (**A**) fine grain structure free from carbides and γ', (**B**) microstructure with intra and intergranular $M_{23}C_6$ and uniform distribution of peak aged of 18 nm dia; and (**C**) microstructure with predominantly intergranular MC and uniform distribution of coarse γ' of 35 nm dia. Microstructure **A** exhibited the highest fatigue resistance while **C** displayed the least. The plastic strain fatigue resistance of **A** and **C** was found to follow the Coffin-Manson relationship while **B** showed a break in Coffin - Manson curve. Two stages corresponding to low and high strain amplitudes in the Coffin-Manson curve were also observed in the cyclic stress - strain curve of **B.** The two stages in Coffin - Manson and cyclic stress - strain curves were attributed to the differences in deformation behaviour occuring at low and high strain amplitudes. Studies carried out on strain rate effects in the range 3×10^{-5} to 3×10^{-2} s^{-1} at 723, 823 and 923K on microstructure A, showed a peak in life at intermediate strain rates. Lower life at higher strain rates was attributed to the increased planarity of slip. Loss of life at the lower end of strain rates investigated was found to result from the deleterious effects of dynamic strain ageing at 723K and 823K, and from the combined influence of time dependent strain accumulation and oxidation at 923K.

KEYWORDS

Nimonic PE16; low cycle fatigue; microstructure; Coffin-Manson curves; cyclic stress-strain curves; dynamic strain ageing; deformation; oxidation.

INTRODUCTION

The gamma Prime (γ')hardened Nimonic PE16 superalloy was developed for applications at elevated temperatures which require good oxidation

resistance and high strength. Despite its widespread use in gas turbine flame tubes, missile hot components, superheater tubes and aircraft ducting systems and nuclear reactors, there is very little information available on its low cycle fatigue behaviour (LCF) (Arbuthnot, 1982; Wahi et al., 1986). Arbuthnot (1982) reported a two slope Coffin-Manson and cyclic stress-strain curve (CSSC) at room temperature, while Wahi et al (1986) have not observed this behaviour in their tests at 773 and 923K on Nimonic PE16. . LCF tests on Nimonic PE16, in three heat treatment conditions, were conducted at 923K, to examine whether the two slope Coffin-Manson and CSSC is typical of the room temperature behaviour or some specific initial microstructural states. In addition, the influence of time and temperature dependent processes on LCF life of solution annealed alloy has been evaluated by performing the tests at 723, 823 and 923K at various strain rates ($\dot{\epsilon}$).

EXPERIMENTAL DETAILS

The chemical composition of the alloy is (wt%): C = 0.07, Ti = 1.20, Al = 1.20, Cr = 16.5 Ni = 43.23, Mo = 3.3, Zr = 0.03, S = 0.004, B = 0.0015, Mn = 0.04, Cu = 0.06 and Fe = 33.83. LCF tests were conducted on Nimonic PE16 in three prior microstructural states. The microstructure A was obtained by solution annealing the alloy at 1313K/4h whereas the microstructures B and C were obtained by subjecting the solution annealed alloy to double ageing treatments at 1073K/2h + 973K/16h and 1173K/1h + 1023K/8h respectively. Double aged microstructures **B** and **C** represented the peak aged and over aged states with respect to γ', while the alloy subjected to solution annealed condition precipitated very fine γ' during equilibration time at 923K before the commencement of the test and represents the under aged state of γ' during LCF testing at 923K. In order to evaluate the influence of microstructure, total strain controlled LCF tests were conducted at $\dot{\epsilon}$ = 3 x 10^{-3} s^{-1}, employing a triangular wave form with strain amplitudes in the range from ± 0.25 to ± 1.25%. A constant strain amplitude of ± 0.6% was used for the tests conducted on solution annealed condition for understanding the $\dot{\epsilon}$ effects in the range 3 x 10^{-5} to 3 x 10^{-2} s^{-1}, and at 723, 823 and 923K. Cylindrical ridge samples of 25 mm gauge length and 10 mm gauge dia were employed for all the tests. Specimen failure life, N_f, was defined as the number of cycles corresponding to 20% fall off in the tensile load recorded at half of the expected fatigue life (Bhanu Sankara Rao et al., 1985). Fractography of the fatigue tested samples was carried out using a Philips 501 scanning electron microscope.

RESULTS AND DISCUSSION

Effects of Microstructure on LCF Behaviour at 923K

Microstructure **A** exhibits higher plastic strain fatigue resistance than the double aged microstructures **B** and **C** (Fig.1). LCF behaviour of **A** and **C** is found to obey Coffin - Manson equation $(\Delta\epsilon_p/2)(2N_f)^c = \epsilon_f'$ relating plastic strain amplitude ($\Delta\epsilon_p/2$) with number of reversals to failure ($2N_f$). However, **B** exhibits a two stage plastic strain amplitude - number of reversals to failure curve (Fig.1). For condition **B**, samples cycled at low strain amplitudes show much shorter lives than would be expected by extrapolation from the high strain amplitude portion of the plot. Table-1 provides the values of constants in Coffin - Manson relationship for the three microstructures. Figures 2a, 2b and 2c show the dependence of cyclic tensile stress on the cycle number and strain amplitude for **A**, **B** and **C**

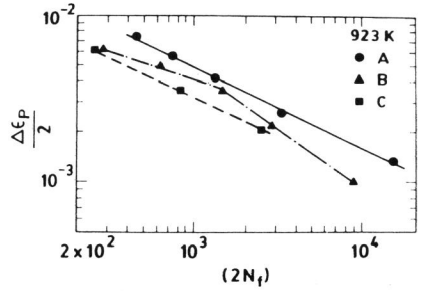

Fig. 1. Coffin-Manson plots for microstructures **A**, **B** and **C** at 923K.

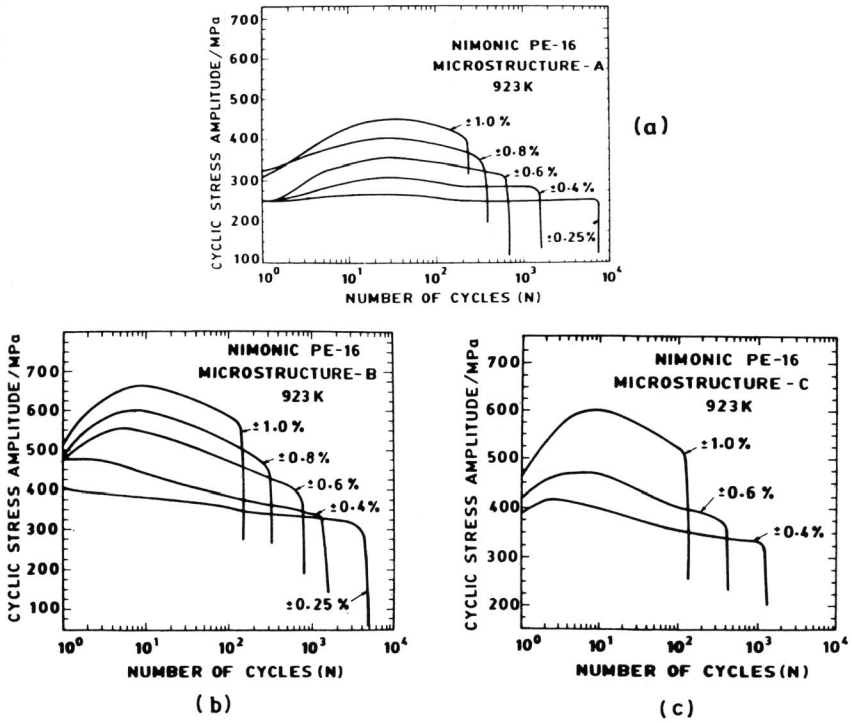

Fig. 2. Cyclic stress response curves of (a) microstructure **A**, (b) microstructure **B** and (c) microstructure **C**.

Table 1. Constants in Coffin-Manson relationship for different metallurgical conditions at 923K

Constants	Microstructure A	B	C
c	0.50	0.32 (high strain) 0.71 (low strain)	0.47
ϵ_f'	0.15		0.08

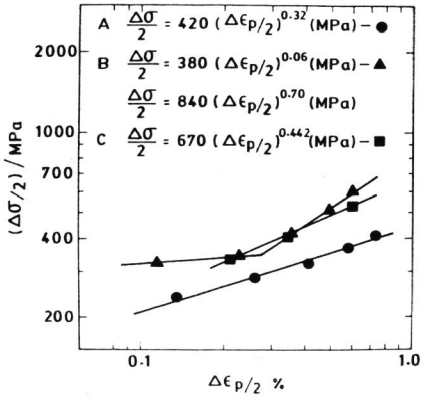

Fig. 3. Half life cyclic stress-strain curves for microstructures **A**, **B** and **C**.

respectively. At high strain amplitudes, the cyclic stress response of all the microstructures is characterized by cyclic hardening to a maximum stress followed by rapid softening to failure. At strain amplitudes $< \pm 0.40\%$, **B** and **C** exhibit a rapid and continuous softening from the begining while **A** shows hardening followed by softening to a saturation stress stage. Cyclic stress strain curves computed at 50% of the number of cycles to failure, are found to obey a power law relationship, $\Delta\sigma/2 = K'(\Delta\epsilon_p/2)^{n'}$ in case of **A** and **C**, while **B** shows two stages in CSSC (Fig.3).Stage 1, at low strain amplitudes is characterised by low work hardening. At high strain amplitudes (stage 2) strain hardening exponent n' increases very sharply.

For microstructure **A**, at all the strain amplitudes, crack initiation is found to occur from the surface in persistent slip bands, subsequently followed by transgranular stage - I and stage-II crack growth mechanisms. The fracture mode in **B** is strain amplitude dependent. At high strain amplitudes transgranular initiation and propagation mechanisms prevailed, while at strain amplitudes less than 0.5% transgranular initiation and mixed mode propagation occurred (Fig.4). Microstructure **C** exhibits by and large a mixed mode fracture at all the strain amplitudes. Comparative evaluation of

striation spacings at equivalent crack lengths under identical testing conditions show the striation spacing in the order, **C > B > A.** Large striation spacings give an indication of higher crack growth rate in **C.**

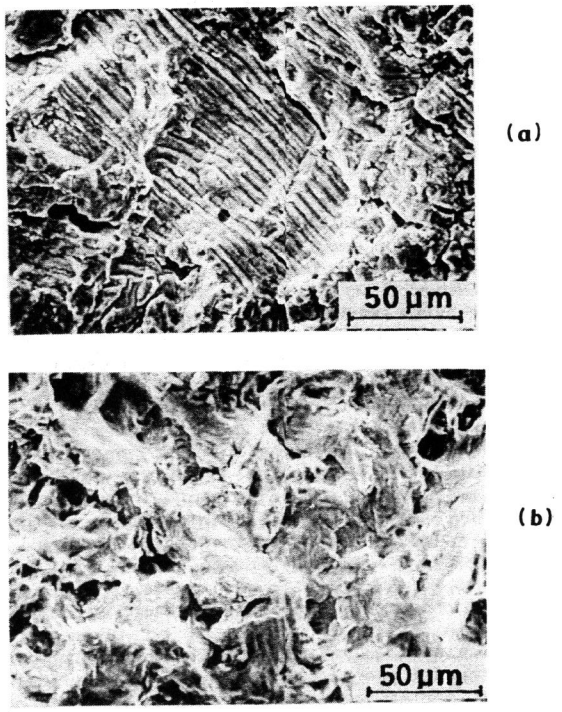

Fig. 4. (a) Transgranular crack propagation in **B** ($\Delta\epsilon_t = \pm 1.0\%$), (b) Mixed mode fracture in **B** ($\Delta\epsilon_t = \pm 0.25\%$).

The existence of discontinuities in a Coffin - Manson curve and corresponding break in CSSC have been reported in nickel base alloys (Arbuthnot, 1982; Lerch and Gerold, 1985) and dual phase steels (Mediratta et al., 1986). The occurrence of two stages in Coffin - Manson plots have been variously attributed to i) the differences in crack propagation modes at low and high strain amplitudes, ii) the enhanced effects of oxidation at low strain amplitudes (Coffin, 1971) and iii) the differences in deformation behaviour at low and high strain amplitudes (Arbuthnot, 1982; Lerch and Gerold, 1985). In the present investigation, we attribute two stage Coffin - Manson and CSSC behaviour to the occurrence of different deformation modes at low and high strain amplitudes.

TEM investigations (Valsan et al., 1987) reveal that microstructure **A** exhibits planar slip character and dislocations move singly in the slip bands at all strain amplitudes. Coarse γ' particles in **C** are found to be by-

passed by the Orowan looping mechanism at all strain amplitudes. In case of **B**, cycling above the critical strain amplitude corresponding to the break points in the Coffin - Manson curve and CSSC produce deformation structures characterized by uniform distribution of dislocations and few dislocation loops around γ'. On the other hand, cycling below the critical strain reveals the formation of planar slip bands, in which the dislocations are mainly paired, indicating indirectly that they are cutting the γ' particles.

Arbuthnot (1982) has also observed the discontinuity in Coffin - Manson and CSSC of peak aged Nimonic PE16 at ambient temperature. Based on TEM studies, it has been suggested that at higher strains the interaction of densely packed slip bands of three different slip systems lead to a break down of planar slip observed at low strain amplitudes. This change in deformation mode as a function of strain amplitude has been considered to be responsible for the change in slopes of the plots. The present results on **B** at 923K also support the change in deformation mode as the cause for two slope behaviour observed in Coffin - Manson and CSSC plots. This is further supported by the fact that no breaks in the plots were observed in **A** and **C** which reveal the same mode of deformation at all strain amplitudes. The plastic strain at which the break in slope occurs has been found to be lower in our tests at compared to that observed at room temperature by Arbuthnot (1982). The decrease in the plastic strain for the break in CSSC at 923K compared to 300K could result from the early onset of slip dispersal mechanisms of climb and cross-slip of dislocations.

The continued cyclic softening in **B** at low strain amplitudes could be attributed to repeated shearing and consequent reduction in size of γ' precipitates in planar slip bands. The observed lower value of n' in stage 1 of CSSC results from reduced work hardening due to particle shearing. The localized deformation in planar slip bands produces large stress concentrations at grain boundaries due to dislocation pile-ups and initiates decohesion at grain boundary carbides, and hence cracking (Srivatsan et al., 1986) as is observed in case of **B** at low strain amplitudes (Fig.4). At low strain amplitudes in **B**, reduction in fatigue life occurs due to early crack nucleation because of the strain localisation in intense slip bands and accelerated propagation in the presence of intergranular cracking. n' values are, however, large in the high plastic strain region. (Fig.3). Higher n' is believed to be caused by homogeneous deformation.

Time Dependent Low Cycle Fatigue in Solution Annealed Condition

The combined influence of temperature and on $2N_f$ is illustrated in Fig.5. Generally, there is a reduction in $2N_f$ with increasing temperature. However, at a given temperature, the life first increases and then falls with decreasing $\dot{\epsilon}$. A peak in life has been reported earlier for single crystal Mar M-200 tested at elevated temperatures in the range 1033-1473K (Leverant and Gell, 1975) and Udimet-700 (Organ and Gell, 1971) tested at 1033K. In this study, analysis of the test data and microstructural investigations reveal that upto four time dependent processes can operate during cyclic deformation in the range of temperatures (723-923K) and $\dot{\epsilon}$ (3×10^{-5} to $3 \times 10^{-2} s^{-1}$) investigated, depending on the test condition.

At highest $\dot{\epsilon}$, for all the temperatures, $2N_f$ is reduced because of the increased planarity of slip, which enabled the formation of intense slip bands at the surface with associated reduction in number of cycles to crack

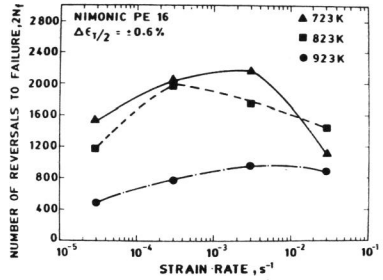

Fig. 5. Temperature and strain rate dependency of fatigue life in **A**.

initiation. The increase in $2N_f$ that occurs at 723 and 823K as the $\dot{\epsilon}$ is initially decreased could result from the onset of dynamic strain ageing (DSA). Two observations provide proof for the occurrence of DSA in this study. During fatigue loading, stress-strain hysteresis loops display serrated flow in the plastic regions at $\dot{\epsilon} = 3 \times 10^{-3} s^{-1}$ and first cycle stress sharply increases with decreasing $\dot{\epsilon}$. The latter observation is a manifestation of the negative strain rate sensitivity of cyclic stress. The serrated flow in stress-strain hysteresis loops, the negative $\dot{\epsilon}$ sensitivity of cyclic stress and large magnitude of cyclic hardening are considered as the manifestations of DSA in LCF (Bhanu Sankara Rao et al., 1986). The increase in fatigue life due to onset of DSA effects could be ascribed to slip dispersal. Plastic strain homogenisation is an effective means to prolong the cyclic life in planar slip materials (Pelloux and Stoltz, 1976) by retarding crack nucleation. The increase in cyclic stress which is required to deform the sample at the imposed strain amplitude in the DSA regime results in the activation of multiple slip, and hence, leads to a more evenly distributed deformation (Bhanu Sankara Rao, 1988). However, the strong DSA which occurs at lower $\dot{\epsilon}$ leads to an eventual decrease in $2N_f$, at 723 and 823K. Under strong DSA conditions intergranular cracking occurs in the bulk of the specimen. This coupled with higher response stresses arising due to DSA would lead to enhanced crack growth rates and reduced life.

At 923K, the decrease in $2N_f$ that results from $\dot{\epsilon}$ decrease is accompanied by a change in crack initiation mode, from transgranular at higher $\dot{\epsilon}$ to intergranular at lower $\dot{\epsilon}$. Decrease in $2N_f$ is caused by the combined effects of time dependent strain accumulation resulting from the dislocation climb and cross slip, and crack initiation occurring at the oxidised grain boundaries connected to the surface. Time dependent strain accumulation is manifested as an incrseased amount of inelastic strain in the total strain controlled cycle, as the $\dot{\epsilon}$ is decreased. Creep damage in the form of wedge cracks or cavities has not been observed in any of the tests.

CONCLUSIONS

1. Nimonic PE16 alloy exhibits higher resistance to cyclic plastic strains in the solution annealed condition while the microstructure containing coarse γ' displays the least at 923K.

2. Plastic strain fatigue resistance of the solution annealed and over aged γ' microstructures are found to follow Coffin-Manson relationship. Microstructure containing γ' in nearly peak aged condition exhibits a break in Coffin - Manson curve. The two stages corresponding to high and low strain amplitudes are also observed in cyclic stress strain curve of peak aged γ' microstructure.
3. The initiation and propagation of cracks occur by transgranular mode in solution annealed condition, while transgranular initiation and mixed mode propagation occur in microstructures containing γ' in peak aged condition at low strain amplitudes and over aged conditions at all strain amplitudes.
4. In the studies of $\dot{\epsilon}$ effects at 723, 823 and 923K in solution annealed condition, it is found that the alloy exhibits a peak in fatigue life at an intermediate $\dot{\epsilon}$. The reduction in life at 723 and 823K at lower $\dot{\epsilon}$ is attributed to DSA effects while at 923K the combined effects of creep deformation and oxidation are found to prevail. The occurrence of intense planar slip caused reduction in life at higher $\dot{\epsilon}$.

ACKNOWLEDGEMENT

The authors wish to thank to Dr.P. Rodriguez, Head, Metallurgy Programme and Materials Science Laboratory for many useful discussions and encouragement. Stimulating discussions with Prof. D.H. Shastry of IISc., Bangalore are gratefully acknowledged.

REFERENCES

Arbuthnot, C.H.D. (1982). The Micro-mechanisms of fatigue deformation in Nimonic PE16. In: Proc. 4th Euro. conf. on fracture (Maurer, K.L. and F.E. Matzer, ed.) Vol.2, pp.407-413. Chameleon, London.

Bhanu Sankara Rao, K., M. Valsan., R. Sandhya., S.K. Ray., S.L. Mannan and P. Rodriguez (1985). Intl. J. Fatigue., 7, 141-147.

Bhanu Sankara Rao, K., M. Valsan., R. Sandhya., S.L. Mannan and P. Rodriguez (1986). High Temperature Materials and Processes, 7, 171-177.

Bhanu Sankara Rao, K. (1988). Influence of metallurgical variables on LCF behaviour of type 304 stainless steel. Ph.D. Thesis, Madras University, India.

Coffin Jr, L.F. (1971). J. Mater., 6, 388.

Lerch, B. and V. Gerold (1985). Acta Metall., 33, 1709-1716.

Leverant, G.R and M. Gell (1975). Metall. Trans., 6A, 367-371.

Mediratta, S.R., V. Ramaswamy and P. Rama Rao (1986). Scripta Metall., 20, 555-558.

Organ, F.E. and M. Gell (1971) Metall. Trans., 2, 943-952.

Pelloux, R.M. and R.E. Stoltz (1976). Proc. Fourth Intl. Conf. on Strength of Metals and Alloys, Vol.3, pp.1023-1036.

Srivatsan, T.S. and E.J. Coyne Jr. (1986). Intl. J. Fatigue., 8, 201-208.

Valsan, M., P. Parameswaran., K. Bhanu Sankara Rao., M. Vijayalakshmi and S.L. Mannan (1987). Micromechanisms of LCF deformation and fracture in Nimonic PE16 superalloy. Presented at 41st Annual Technical Meeting of IIM., 12-14 Nov., Trivandrum, India.

Wahi, R.P., V.V. Kutumba Rao., H.M. Yun and W. Chen (1987). LCF behaviour of Nimonic PE16 at temperatures upto 650°C, In: Low Cycle Fatigue and Elasto-Plastic Behaviour of Metals (K.T. Rie, ed.), pp.290-295. Elsevier Applied Science, London.